HHS Public Access

Author manuscript

Dev Biol. Author manuscript; available in PMC 2020 October 15.

Published in final edited form as:

Dev Biol. 2019 October 15; 454(2): 108–117. doi:10.1016/j.ydbio.2019.06.019.

Dnmt1 is required for proximal-distal patterning of the lung endoderm and for restraining alveolar type 2 cell fate

Derek C. Liberti[1,2,3,*], **Jarod A. Zepp**[2,3,*], **Christina A. Bartoni**[2,3], **Kyle H. Liberti**[4], **Su Zhou**[3], **Minmin Lu**[3], **Michael P. Morley**[2,3], **Edward E. Morrisey**[1,2,3,5,6]

[1]Department of Cell and Developmental Biology, Perelman School of Medicine, University of Pennsylvania, Philadelphia, PA 19104

[2]Penn Cardiovascular Institute, University of Pennsylvania, Philadelphia, PA 19104

[3]Penn Center for Pulmonary Biology, University of Pennsylvania, Philadelphia, PA 19104

[4]Engineering, Red Hat, Raleigh, NC 27601

[5]Department of Medicine, University of Pennsylvania, Philadelphia, PA 19104

[6]Penn-CHOP Lung Biology Institute, Perelman School of Medicine, University of Pennsylvania, Philadelphia, PA 19104

Abstract

Lung endoderm development occurs through a series of finely coordinated transcriptional processes that are regulated by epigenetic mechanisms. However, the role of DNA methylation in regulating lung endoderm development remains poorly understood. We demonstrate that DNA methyltransferase 1 (Dnmt1) is required for early branching morphogenesis of the lungs and for restraining epithelial fate specification. Loss of *Dnmt1* leads to an early branching defect, a loss of epithelial polarity and proximal endodermal cell differentiation, and an expansion of the distal endoderm compartment. Dnmt1 deficiency also disrupts epithelial-mesenchymal crosstalk and leads to precocious distal endodermal cell differentiation with premature expression of alveolar type 2 cell restricted genes. These data reveal an important requirement for Dnmt1 mediated DNA methylation in early lung development to promote proper branching morphogenesis, maintain proximal endodermal cell fate, and suppress premature activation of the distal epithelial fate.

Address correspondence to: Edward E. Morrisey, Ph.D., University of Pennsylvania, Translational Research Center, Room 11-124, 3400 Civic Center Boulevard, Building 421, Philadelphia, PA 19104-5129, Phone: 215-573-3010, Fax: 215-573-2094 emorrise@pennmedicine.upenn.edu.

*These authors contributed equally to this work.

Author Contributions

D.C.L., J.A.Z., and E.E.M. designed the experiments and wrote the manuscript; D.C.L., J.A.Z., C.A.C., S.Z., and M.L. performed experiments; D.C.L., J.A.Z., C.A.C., K.H.L. and E.E.M. analyzed data; M.P.M. performed bioinformatic analysis.

Introduction

The lung endoderm is initially specified from a small number of NK2 homeobox 1 (Nkx2.1) expressing cells within the ventral anterior foregut endoderm. These Nkx2.1+ endoderm cells give rise to the entirety of lung epithelium and are patterned in a proximal-distal fashion in part through a process called branching morphogenesis. Throughout this temporally regulated process, early endodermal precursors undergo fate decisions along the highly patterned proximal-distal axis (Hines and Sun, 2014; Swarr and Morrisey. 2015; Whitsett et al., 2019). This patterning serves to spatially restrict proximal from distal epithelial progenitors. Proximal epithelial precursors, marked by expression of SRY-box 2 (Sox2), will give rise to airway lineages, such as ciliated and secretory cells. The distal epithelial precursors, marked by SRY-box 9 (Sox9), will ultimately give rise to alveolar lineages, alveolar type 1 (AT1) and type 2 (AT2) cells, which form the surface for gas exchange and produce pulmonary surfactant respectively. Branching morphogenesis and cell fate specification are critical for the proper formation of the mature lung, and perturbations in either of these processes can result in rapid perinatal distress or lethality.

Epigenetic mechanisms of gene regulation have been previously shown to play critical roles in lung development. Previously, we have demonstrated that chromatin modifying enzymes histone deacetylases 1 and 2 (HDAC1/2) are required in the lung epithelium to maintain expression of *Sox2* and, subsequently, for proximal airway development (Wang et al., 2013). Additionally, histone deacetylase 3 (HDAC3) regulates AT1 cell spreading, which is required for distal alveolar maturation (Wang et al., 2016a; Wang et al., 2016b). Further, the Ezh2 component of the Polycomb repressive complex 2 (PRC2) plays an essential role in the development of both epithelial and mesenchymal lineages, where it represses the basal cell lineage fate in the epithelium and constrains the smooth muscle cell fate in the mesoderm (Snitow et al., 2016; Snitow et al., 2015).

DNA methylation has been shown to be a critical regulator of cell differentiation in multiple organs, including the prostate, intestine, kidney, and brain. Loss of *Dnmt1* in these organs has been shown to induce both precocious differentiation and a loss of proper morphogenesis (Elliott et al., 2015; Fan et al., 2005; Joseph et al., 2019; Li et al., 2019; Sheaffer et al., 2014; Takizawa et al., 2001). DNA methyltransferase 1 (Dnmt1) acts both as a *de novo* and maintenance methyltransferase, and it is required for embryonic development as *Dnmt1* null mice exhibit developmental arrest by E9.5, resulting in lethality before E11.0 (Li et al., 1992). Despite its clear importance in organ development, the specific role of Dnmt1 in regulating lung development is unknown.

In this study, we demonstrate that epithelial Dnmt1 is required for lung morphogenesis and for epithelial fate specification. Epithelial branching defects appear in *Dnmt1* deficient lungs as early as E11.5. As morphogenesis progresses, *Dnmt1* deficient lungs fail to branch properly, leading to the formation of cystic sacs and lung hypoplasia. We show that Dnmt1 is required to maintain proximal-distal patterning and that loss of *Dnmt1* expression in the epithelium results in the expansion of the distal compartment with a concomitant loss of proximal endoderm cell fate and the disruption of epithelial polarity and epithelial-mesenchymal crosstalk. Dnmt1 also acts to restrain distal epithelial cell differentiation with

loss of *Dnmt1* leading to precocious AT2 cell fate gene expression in the early lung endoderm. These data show that Dnmt1 plays a critical role in defining the proximal-distal patterning of the lung endoderm and is essential in restricting the AT2 cell fate early in lung development.

Results

Loss of Dnmt1 from lung endoderm leads to lung hypoplasia

To begin defining the role of DNA methylation during lung endoderm development, we examined the expression of *Dnmt1*, a major de novo and maintenance DNA methylation factor. Analysis of mouse lung epithelial RNA-seq data shows that Dnmt1 is highly expressed in the embryonic day (E12.5) lung endoderm compared to the adult lung epithelium (Fig. 1A) (Herriges et al., 2014). Immunostaining for Dnmt1 protein demonstrates that it is present throughout the mesoderm and endoderm (Fig. 1B). To test the importance of Dnmt1 in lung development, we inactivated *Dnmt1* in the lung endoderm by generating Shh^{Cre}:$Dnmt1^{Flox/Flox}$ ($Dnmt1^{EKO}$) mice (Fig. 1C). At E14.5, $Dnmt1^{EKO}$ lungs are hypoplastic, and by E18.5 the airways become dilated and cystic in appearance (Figs. 1D and 1E). These data demonstrate that Dnmt1 is expressed at high levels in both the developing lung endoderm and mesoderm, and its expression in the endoderm is essential for normal lung development.

Endodermal loss of Dnmt1 disrupts proximal-distal patterning

To examine the effect of loss of *Dnmt1* on the developing lung, cell death and proliferation were assessed. Loss of Dnmt1 protein was confirmed at E14.5, and this loss was accompanied by both an increase in apoptotic endodermal cells and a significant decrease in proliferating cells (Figs. 2A, 2B, and 2C). Epithelial identity is at least partially preserved in $Dnmt1^{EKO}$ mutants as they continue to express Nkx2.1 (Fig. 2D). However, epithelial shape and possibly polarity appeared dysregulated in $Dnmt1^{EKO}$ mutants as evidenced by aberrant Cadherin 1 (Cdh1) staining at E14.5 (Fig. 2C). We next assessed whether smooth muscle and endothelial cells were present and properly localized in $Dnmt1^{EKO}$ mutants. Transgelin (Tagln), also known as SM22a, immunostaining revealed that while there was less smooth muscle present in $Dnmt1^{EKO}$ lungs, it continued to encircle large vessels and proximal airways as in control lungs (Fig 2D). Additionally, platelet and endothelial cell adhesion molecule 1 (Pecam1) immunostaining indicated vascularization of $Dnmt1^{EKO}$ lungs (Fig 2D). To determine whether proximal-distal patterning was affected in $Dnmt1^{EKO}$ lungs, expression of the critical transcriptional regulators Sox2 and Sox9 was assessed. These analyses indicate that proximal-distal patterning of the lung endoderm is disrupted with reduced Sox2 expression and expanded Sox9 expression (Fig. 2E). However, Sox9 expression in cartilage precursors appeared to be normal (Fig. 2E). Similar results were obtained with forkhead box protein P2 (Foxp2), a marker of distal endoderm, and stage-specific embryonic antigen-1 (SSEA1), a marker of proximal endoderm (Fig. 2D) (Shu et al., 2001). These observations indicate that loss of *Dnmt1* results in increased cell death, decreased proliferation, and impaired patterning of the proximal-distal endoderm axis in the developing lung.

Dnmt1 is essential to maintain epithelial-mesenchymal crosstalk and epithelial polarity

After observing defects in both proximal distal patterning and epithelial shape, we next investigated how loss of *Dnmt1* impacts epithelial-mesenchymal crosstalk and polarity (Fig. 3A). To determine whether epithelial-mesenchymal crosstalk is impacted in Dnmt1^{EKO} lungs, we performed RNA fluorescence *in situ* hybridization for genes known to be essential for guiding branching morphogenesis. Fibroblast growth factor (Fgf) signaling is known to play a key role in branching morphogenesis by driving growth of the budding endodermal tips of the developing lung (Abler et al., 2009; Kadzik et al., 2014; Lebeche et al., 1999; Weaver et al., 2000). We found that *Fgfr2* expression was decreased in Dnmt1^{EKO} lungs compared to control, suggesting that the Dnmt1 mutant endoderm was less receptive to branching signals from the mesoderm (Fig. 3B). Additionally, *Fgf10* expression appeared increased and expanded (Fig. 3B). Sonic hedgehog (Shh) and bone morphogenetic protein 4 (Bmp4) are also critical signaling factors that regulate branching morphogenesis. While *Shh* is expressed throughout the developing endoderm, it is enriched at budding tips where it is thought to suppress Fgf signaling to promote bifurcation of developing lung buds along with *Bmp4*, which is typically restricted to the distal compartment (Kadzik et al., 2014; Lebeche et al., 1999; Litingtung et al., 1998; Miller et al., 2001; Pepicelli et al., 1998; Weaver et al., 2000). Analysis of *Bmp4 and Shh* expression in Dnmt1^{EKO} lungs revealed they were enriched throughout the endoderm, consistent with our previous observation of the expansion of the distal compartment (Fig. 3B). These data suggest that loss of endodermal *Dnmt1* disrupts the epithelial-mesenchymal signaling required for proper branching morphogenesis.

To assess whether epithelial polarity was disrupted in Dnmt1^{EKO} lungs, we examined the localization of cell surface and polarity associated proteins. β-catenin immunostaining revealed abnormal epithelial cell shape in Dnmt1 mutant lungs compared to controls (Fig. 3C). Immunostaining for zonula occludens-1 (ZO-1), which is typically restricted to the apical membrane, revealed aberrant localization in the Dnmt1 mutant epithelial cells to both the lateral and basal membranes in addition to the apical membrane (Fig. 3D). Dnmt1^{EKO} lungs also exhibit ectopic localization of Cdh1 to the apical surface of mutant epithelial cells and a loss of the columnar shape characteristic of normal distal epithelium (Fig. 3E). Discs large homolog 1 (Dlg1) expression is primarily restricted to the basal membrane of normal developing lung endodermal cells, but in Dnmt1^{EKO} lungs expression was observed at the basal membrane, within the cytoplasm, and on the lateral cell membrane (Wan et al., 2013) (Fig. 3F). Similarly, while laminin was found properly deposited in the basement membrane of Dnmt1^{EKO} lungs, it also appeared aberrantly localized throughout the endoderm of Dnmt1 mutants (Figs. 3D and 3F). The presence of detached clusters of cellular debris in the luminal space of Dnmt1 mutant endodermal buds is also readily apparent, indicating a sloughing off of cells, consistent with a loss of polarity and increased apoptosis (Figs. 2C–E, 3D, and 3F). These data suggest that loss of endodermal *Dnmt1* perturbs both epithelial-mesenchymal crosstalk and epithelial polarity leading to improper branching and to the formation of deformed, cystic lung buds.

Dnmt1 activity is required for proximal endoderm differentiation in the lung

We next sought to determine whether endodermal loss of *Dnmt1* results in a failure of lung epithelial fate determination. Dnmt1^{EKO} mutant lung tissue at E18.5 is highly dysplastic with a cystic appearance (Fig. 4A). Immunostaining for Nkx2.1 indicated that Dnmt1^{EKO} mutants continue to express Nkx2.1 in the endodermal lining of the dysplastic airways (Figs. 4A and 4C). Expression of Tagln and Pecam1 immunostaining was observed in Dnmt1^{EKO} mutants with the large cystic structures surrounded by smooth muscle (Fig. 4B). There was almost a complete loss of proximal epithelial cells as noted by a dramatic loss of by forkhead box J1 (Foxj1) and secretoglobin family 1A member 1 (Scgb1a1) expressing cells (Fig. 4C). Intriguingly, the distal lung AT1 and AT2 epithelial cell fates appeared to be present in Dnmt1^{EKO} animals, as cells expressing either Hopx or Sftpc were observed (Fig. 4C). These data suggest that Dnmt1 regulates the differentiation of proximal epithelial cells from the Nkx2.1 expressing early endodermal lung progenitors.

Dnmt1 is required for branching morphogenesis

Our data suggest an expansion of distal Sox9+ epithelial cell fates and a commensurate loss of Sox2+ proximal cells in Dnmt1^{EKO} mutant lungs. Previous work has shown that perturbations in the proximal-distal axis due to loss or gain of Sox9 expression in the lung endoderm result in cystic appearing distal tips (Rockich et al., 2013). To assess the changes in branching morphogenesis, we examined Dnmt1^{EKO} mutant lungs at E12.5. Dnmt1 protein loss is clear at E12.5, and there is a subtle defect in Dnmt1^{EKO} lungs by H&E staining (Figs. 5A and 5B). Sox2 and Sox9 expression are not significantly altered in E12. 5 Dnmt1^{EKO} lungs (Fig. 5C).

Consistent with the lack of proximal-distal perturbations at E12.5, we did not observe a significant defect in proliferation of the epithelium in the Dnmt1^{EKO} lungs (Fig. 5D). However, whole mount imaging revealed that at E12.5 there was defective lateral domain branching in Dnmt1^{EKO} lungs (Fig. 5E). Due to the subtle branching defect observed at E12.5, we next tested whether loss of *Dnmt1* leads to progressive impairment in branching morphogenesis, thus impacting proximal-distal patterning. We utilized time-lapse imaging using control and Dnmt1^{EKO} mutant lungs harvested at E11.5 and cultured as explants as previously described (Carraro et al., 2010; Del Moral and Warburton, 2010; Kadzik et al., 2014; Schnatwinkel and Niswander, 2013). Imaging these lung explants for 72 hours reveals a severe impairment of branching in the Dnmt1^{EKO} lungs compared to the littermate controls (Fig. 5F and Movie S1 and S2). By the end of the time-lapse experiment, the Dnmt1^{EKO} lungs were dysmorphic in appearance and lacked the highly iterative branching observed in the controls. This explant experiment serves to uncouple the interaction of the lung with other organs that may also be affected by loss of Dnmt1 due to expression of Shh^{Cre}, which could in turn impact lung development, showing that the observed phenotype is lung intrinsic. To investigate the potential effect of loss of Dmnt1 in other organs expressing Shh^{Cre}, we examined the developing gut at E12.5 and 14.5. Immunohistochemical staining for Dnmt1 confirmed loss of Dnmt1 protein at these timepoints (Supp. Fig. 1). However, H&E as well as immunohistochemistry for Cdh1 demonstrated no obvious morphological defects consistent with a previous report (Supp. Fig. 1)(Elliott et al., 2015). Together, these data indicate that loss of Dnmt1 leads to

progressive failure of lung development due to defects in both branching morphogenesis as well as proximal-distal patterning of the lung endoderm.

Endodermal Dnmt1 activity represses the distal alveolar type 2 cell fate

To determine the transcriptional targets of Dnmt1 mediated repression, we isolated lungs at E12.5 from Dnmt1^{EKO} and littermate controls and performed RNA sequencing (RNA-seq). E12.5 was chosen to reduce secondary and tertiary gene expression changes due to the major phenotypic defects observed in Dnmt1^{EKO} mutant lungs at later time points. Principal component analysis revealed distinct gene expression changes due to loss of *Dnmt1* expression (Fig. 6A). Intriguingly, differential gene expression analysis revealed de-repression of distal lung epithelial expressed genes including inhibitor of DNA binding 2 (*Id2*) and surfactant proteins A1, B, and C (*Sftpa1, Sftpb, and Sftpc)* (Figs. 6B–6D and Supp. Table 1). Gene ontology of the top differentially expressed genes included de-repression of genes associated with Hedgehog signaling and alveolar lamellar body formation (Fig. 6D). Further examination indicated that a number of known AT2 cell specific transcripts were upregulated in the Dnmt1^{EKO} tissue based on the RNA-seq data (Fig. 6D). We confirmed that *Dnmt1* expression was reduced and *Sftpc* was highly up-regulated in the Dnmt1^{EKO} mutants by quantitative real-time PCR (Q-PCR) (Fig. 6E). Moreover, immunostaining revealed rare epithelial cells expressing Sftpc and Sftpb protein in Dnmt1^{EKO} at E12.5, which became more abundant by E14.5. Sftpc and Sftpb protein were not detected in Dnmt^{control} lungs at E12.5. Sftpb protein was observed in control littermate lungs at E14.5, but expression was restricted to the distal endoderm (Fig. 6F). In contrast, Sftpb expression in Dnmt1^{EKO} lungs was localized throughout the endoderm, consistent with the precocious expansion of the distal endoderm phenotype in these mutants (Fig. 6F). Taken together, these data suggest that loss of *Dnmt1* results in precocious differentiation of early Sox9-positive epithelial precursors towards a more terminal distal fate, specifically the AT2 cell.

Discussion

The role of epigenetic factors in regulating lung branching morphogenesis and epithelial cell fate specification remain poorly understood. Our data revealing the importance of Dnmt1 in regulating both proximal-distal endoderm patterning as well as suppressing genes specific for the AT2 cell fate, indicates the necessity of DNA methylation for these basic cellular processes during lung development. The precocious activation of genes restricted to AT2 cells upon deletion of Dnmt1 suggests an important role for DNA methylation in the correct temporal activation of specific transcriptional programs during lung development.

Previous reports of the relationship between branching morphogenesis and proximal-distal patterning of the airways suggest a connection between these two processes (Alanis et al., 2014; Chang et al., 2013). Our data support this concept as precocious differentiation in *Dnmt1* deficient endoderm correlates with defective branching. However, the exact mechanistic interaction between these two processes is unclear. Interestingly, previous studies examining other epigenetic regulatory pathways during lung development have also revealed a loss of early proximal-distal patterning of the endoderm. Combined loss of

histone deacetylates (HDAC) 1 and 2 in the developing lung endoderm also led to a decrease in Sox2 expressing proximal endoderm progenitors (Wang et al., 2013). Additionally, this study showed an increase in certain distal lung endoderm paracrine signaling factors, such as Bmp4, consistent with our data. A different study revealed that loss of Sin3a, a component of the NuRD chromatin remodeling complex, also led to decreased proximal lung endoderm development (Yao et al., 2017). The similarity between these two studies and those presented in the current report suggest a particular sensitivity of proximal lung endoderm development to epigenetic perturbation. Whether these three pathways converge on a common epigenetic regulatory node to cause such a phenotype will require further investigation.

The interaction between Fgf, Bmp, and Shh signaling is essential for early lung development. While few genes are down-regulated at E12.5 in $Dnmt^{EKO}$ lungs, patched 1 (Ptch1) is of particular interest because it a direct target of Shh signaling and has been suggested to pattern Fgf10 expression during branching morphogenesis (Fig. 6C)(Abler et al., 2009; Ho and Wainwright, 2017). *Ptch1* expression is thought to be a direct readout of Shh signaling (Abler et al., 2009). Moreover, it has been suggested that early ablation of mesodermal Ptch1 leads to spatial restriction of *Fgf10* expression (Ho and Wainwright, 2017). However, our data show that both *Shh* and *Fgf10* expression are expanded in E14.5 $Dnmt^{EKO}$ lungs despite down-regulation of *Ptch1* at E12.5 (Fig. 3B and 6C). This data suggests that *Ptch1* down-regulation at E12.5 indicates a defect in Dnmt1 mutant mesodermal receptivity to Shh, limiting Shh signaling from the endoderm to the mesoderm. Loss of Ptch1 could also be reinforced by down-regulation of endodermal Fgfr2, which is known to negatively impact Ptch1 expression and branching morphogenesis (Fig. 3B)(Abler et al., 2009). Previous examination of Shh null mice revealed that loss of Shh leads to an expansion of *Fgf10* expression in the lung mesoderm and increased *Bmp4* expression in the endoderm, consistent with our results (Pepicelli et al., 1998). Moreover, because Fgf10 is known to induce *Bmp4* expression, as *Fgf10* expression expands unrestricted to surround the developing endoderm, it could further upregulate *Bmp4*, inhibiting proximal endoderm specification consistent with the expansion of the distal endoderm at the cost of the proximal that we observe in $Dnmt1^{EKO}$ lungs (Lebeche et al., 1999; Weaver et al., 2000). Additionally, expansion of Bmp4 and Shh and loss of Fgfr2 in the endoderm would in turn perturb receptivity of the endoderm to the increased Fgf10 signal from the mesoderm leading to the improper expansion and branching seen in Dnmt1 mutant lungs. Further studies aimed at uncovering how epigenetic mechanisms regulating endoderm development impact epithelial-mesenchymal crosstalk will be invaluable to our understanding of how early patterning is maintained throughout development.

DNA methylation is required to restrain differentiation in early embryos (Hargan-Calvopina et al., 2016; Sen et al., 2010). Moreover, loss of the *de novo* and maintenance methylation factor Dnmt1 in the early embryo and in organs, such as the intestine, brain, and skin, leads to precocious differentiation, which is consistent with our findings in the lung (Elliott et al., 2015; Fan et al., 2005; Hargan-Calvopina et al., 2016; Sen et al., 2010; Takizawa et al., 2001). Remarkably, loss of Dnmt1 consistently correlates with reactivation of primordial germ cell restricted genes such as Dazl, Sohlh2, Tex19.1, Pet2, genes of the reproductive homeobox (Rhox) cluster Gm9, Rhox2a, Rhox2f, Rhox2d, and genes expressed in the germ

line of the early embryo 4930550L24Rik, Mov10l1, Tex13, Rpl39l, Rpl10l, Tuba3a, Tuba3b (Arand et al., 2012; Auclair et al., 2014; Bergsagel et al., 1992; Borgel et al., 2010; Branco et al., 2016; Chen et al., 2014; Crichton et al., 2017; Hackett et al., 2012; Hargan-Calvopina et al., 2016; Li et al., 2019; Maatouk et al., 2006; Shin et al., 2017; Tsui et al., 2000). Our RNA-seq analysis shows that these genes are among the most differentially expressed in $Dnmt1^{EKO}$ lungs compared to control lungs. Together, these data suggest that Dnmt1 is required in multiple organs to suppress aberrant gene expression to allow proper cell differentiation and morphogenesis to proceed. Further study is necessary to understand whether and how reactivation of these genes associated with early embryonic development may direct precocious differentiation toward a particular cell fate.

Lung morphogenesis and differentiation in the early embryo are maintained by a precise temporal and spatially restricted developmental program. Our understanding of how proximal-distal patterning is achieved and maintained in the developing lung, despite scores of elegant studies, remains limited. Our results show that loss of *Dnmt1* in the epithelium leads to loss of proximal endoderm development, defects in branching morphogenesis, epithelial polarity, and epithelial-mesenchymal crosstalk, and premature activation of the AT2 cell transcriptional program. Together with other work examining epigenetic regulation of lung development, our study suggests that endodermal differentiation during lung development requires specific epigenetic cues that promote the development of the proper ratio of proximal and distal progenitor cells from the multipotent early lung endoderm.

Materials and Methods

Animals

The information related to the generation and genotyping of the $Dnmt1^{flox}$,Shh^{cre}, $R26^{RCFL\text{-}TdTom}$ mouse lines have been previously described (Harfe et al., 2004; Jackson-Grusby et al., 2001; Madisen et al., 2015). The mice used for this study were purchased from Jackson Laboratories and were maintained on a mixed background. Animal procedures were completed under the guidance of the University of Pennsylvania Institutional Animal Care and Use Committee. Shh^{Cre}:$Dnmt1^{Flox/+}$ littermates ($Dnmt^{control}$) were used as controls for all experiments unless specifically noted in figures as control, indicating littermate wildtype controls were used. At least three biological replicates were used for all experiments.

Histology, Immunohistochemistry, and RNA FISH

Whole embryos were fixed in 2% paraformaldehyde overnight, dehydrated with a series of ethanol washes (30%, 50%, 70%, 95%, and 100%), embedded in paraffin wax, and sectioned at a thickness of 6–8μm. Standard procedures were employed for Hematoxylin and eosin (H&E) staining.

Immunohistochemistry was performed with the following antibodies: Dnmt1 (rabbit, Novus, nb100–264, 1:500), Ttf1 (Nxk2.1) (rabbit, Santa Cruz, sc-13040, 1:50) Foxj1 (mouse, eBioscience, 14-9965-80, 1:250), Scgb1a1 (rabbit, Santa Cruz, sc-9772, 1:20), Hopx (mouse, Santa Cruz, sc-398703, 1:200), Sftpc (rabbit, Millipore, ab3786, 1:100), Sftpb (rabbit, Abcam, ab40876, 1:500), Phosphohistone H3 (mouse, Cell Signaling, 9706L,

1:200), Cdh1 (E-cadherin) (rabbit, Cell Signaling, 3195S, 1:100), Sox2 (goat, Santa Cruz, sc-17320, 1:10), Sox9 (rabbit, Santa Cruz, sc-20095, 1:50), Foxp2 (rabbit antisera, 1:50), Ssea1 (mouse, Millipore, mab4301, 1:100), Tagln (Sm22a) (goat, Abcam, ab10135, 1:50), Pecam1 (rat, HistoBioTec, dia-310, 1:200), β-catenin (mouse, BD Biosciences, 610154, 1:25), Zo-1 (mouse, Thermo Fisher, 33–9100, 1:100), SAP-97 (Dlg1) (mouse, Santa Cruz, sc-9961, 1:50), Laminin (rabbit, Sigma Aldrich, L9393, 1:200).

RNA FISH was performed using RNAscope probes as indicated by the manufacturer (Advanced Cell Diagnostics). The following RNAscope probes were used: Mm-Fgfr2-no-XHs (Advanced Cell Diagnostics, catalog# 443501), Mm-Fgf10-C2 (Advanced Cell Diagnostics, catalog# 446371-C2), Mm-Bmp4-C1 (Advanced Cell Diagnostics, catalog# 401301), and Mm-Shh-C2 (Advanced Cell Diagnostics, catalog# 314361-C2).

Representative images from stained slides were acquired using either a Nikon Eclipse Ni widefield microscope, including processing with NIS-Elements Advanced Research deconvolution software, or a Zeiss LSM 710 confocal microscope. Lungs used for the whole mount images were dissected in phosphate buffered saline (Corning), fixed in 2% paraformaldehyde (Thermo Fisher) overnight, and imaged on a Leica TCS SP8 confocal microscope.

Quantitative analysis

The proportion of proliferating epithelial cells was determined by immunostaining for Cdh1 and Phosphohistone H3. Images were captured using a Zeiss LSM 710 confocal microscope. At least 500 cells from equivalent structures were counted per mouse using ImageJ software. Researchers were blinded to the identity of samples during counting. Branch point analysis was performed using Imaris software.

RNA Sequencing and Analysis

RNA was extracted with Trizol (Life Technologies) from snap-frozen embryonic day 12.5 mutant and littermate lungs. Library prep with PolyA selection and ultra-low input RNA-seq library preparation was performed by GeneWiz, LLC. Fastq files were evaluated for quality with the FastQC program and subsequently aligned against the mouse reference genome (mm9) using the STAR aligner (Dobin et al., 2013). Duplicate reads, flagged with the MarkDuplicates program from Picard tools, were excluded from analysis. Read counts per gene for Ensembl (v67) gene annotations were computed using the Rsubread R package. Gene counts represented as counts per million (CPM) were nominalized using TMM method in the edgeR R package, and genes with 25% of samples with a CPM < 1 were deemed low expressed and removed. The data were transformed with the VOOM function from the limma R package to generate a linear model to perform differential gene expression analysis (Law et al., 2014). Given the small sample size of the experiment, we employed the empirical Bayes procedure as implemented in limma to adjust the linear fit and to calculate P values. P values were adjusted for multiple comparisons using the Benjamini-Hochberg procedure. Plots as shown in Figure 5 were generated in R, and GO enrichment analysis was performed using the GAGE R package. The Gene Expression Omnibus number for the RNA-seq data is GSE129177.

Live imaging

Explants were cultured as previously described with slight modification (Carraro et al., 2010; Del Moral and Warburton, 2010). Briefly, lungs were dissected from E11.5 embryos in cold PBS and placed on 0.4μm pore transwell inserts in DMEM/F12 (Gibco) supplemented with Antibiotic-Antimycotic (Gibco). Lungs were imaged using the EVOS FL Auto 2 Imaging System, cultured on an incubated stage at 37°C and 5% CO_2, and imaged every hour for 3 days.

Statistical analysis

Statistical tests were performed in Prism 7. A student's t-test was performed to compare experimental groups. A difference between groups was considered statistically significant if $P < 0.05$.

qPCR

RNA was extracted from whole lungs at E12.5 by Trizol (Life Technologies) isolation. Synthesis of cDNA was performed using a QuantiTect Whole Transcriptome Kit (Qiagen). Three biological replicates were used for all experiments and were from the same samples used for RNA-seq analysis. Data were normalized to GAPDH. Data are represented by mean ± SEM. Quantitative real-time PCR was performed using SYBR Green (Applied Biosystems) on a QuantStudio 7 Flex using the following primer sets:

qPCR Primers		
Target Gene	**Forward Primer (5'-3')**	**Reverse Primer (5'-3')**
Gapdh	AGGTTGTCTCCTGCGACTTCA	CCAGGAAATGAGCTTGACAAAGTT
Nkx2.1	ATGGTACGGCGCCAACCCAGA	CATGCCACTCATATTCATGCCGCT
Sox2	TGCACATGGCCCAGACTA	TTCTCCAGTTCGCAGTCCAG
Sox9	CGGCTCCAGCAAGAACAAG	GCGCCCACACCATGAAG
Dnmt1	ATCCTGTGAAAGAGAACCCTGT	CCGATGCGATAGGGCTCTG
Sftpc	AGCAAAGAGGTCCTGATGGAGAGT	CACAACCACGATGAGAAGGCGTTT

Supplementary Material

Refer to Web version on PubMed Central for supplementary material.

Acknowledgements

This work was supported by funding from the National Institutes of Health (R01-HL132999, R01-HL087825, U01-HL134745, and U01-HL110942 to E.E.M.; T32-HL007586 to J.A.Z.; T32-HD083185 to D.C.L.). The authors would like to acknowledge the members of the Morrisey laboratory for helpful discussion and technical assistance, in particular Dr. David Frank, Madison Kremp, Yun Ying, and Dr. Shanru Li. The authors thank Apoorva Babu for assistance with RNA-Seq data processing and associated graph generation. The authors are also grateful for the technical assistance provided by the Penn Cardiovascular Histology Core for their histological services and to the Cell and Developmental Biology Microscopy Core of the Perelman School of Medicine for their assistance with confocal microscopy.

References

Abler LL, Mansour SL, Sun X, 2009 Conditional gene inactivation reveals roles for Fgf10 and Fgfr2 in establishing a normal pattern of epithelial branching in the mouse lung. Dev Dyn 238, 1999–2013. [PubMed: 19618463]

Alanis DM, Chang DR, Akiyama H, Krasnow MA, Chen J, 2014 Two nested developmental waves demarcate a compartment boundary in the mouse lung. Nat Commun 5, 3923. [PubMed: 24879355]

Arand J, Spieler D, Karius T, Branco MR, Meilinger D, Meissner A, Jenuwein T, Xu G, Leonhardt H, Wolf V, Walter J, 2012 In vivo control of CpG and non-CpG DNA methylation by DNA methyltransferases. PLoS genetics 8, e1002750. [PubMed: 22761581]

Auclair G, Guibert S, Bender A, Weber M, 2014 Ontogeny of CpG island methylation and specificity of DNMT3 methyltransferases during embryonic development in the mouse. Genome biology 15, 545. [PubMed: 25476147]

Bergsagel PL, Timblin CR, Eckhardt L, Laskov R, Kuehl WM, 1992 Sequence and expression of a murine cDNA encoding PC326, a novel gene expressed in plasmacytomas but not normal plasma cells. Oncogene 7, 2059–2064. [PubMed: 1408147]

Borgel J, Guibert S, Li Y, Chiba H, Schubeler D, Sasaki H, Forne T, Weber M, 2010 Targets and dynamics of promoter DNA methylation during early mouse development. Nat Genet 42, 1093–1100. [PubMed: 21057502]

Branco MR, King M, Perez-Garcia V, Bogutz AB, Caley M, Fineberg E, Lefebvre L, Cook SJ, Dean W, Hemberger M, Reik W, 2016 Maternal DNA Methylation Regulates Early Trophoblast Development. Dev Cell 36, 152–163. [PubMed: 26812015]

Carraro G, del Moral PM, Warburton D, 2010 Mouse embryonic lung culture, a system to evaluate the molecular mechanisms of branching. J Vis Exp.

Chang DR, Martinez Alanis D, Miller RK, Ji H, Akiyama H, McCrea PD, Chen J, 2013 Lung epithelial branching program antagonizes alveolar differentiation. Proc Natl Acad Sci U S A 110, 18042–18051. [PubMed: 24058167]

Chen HH, Welling M, Bloch DB, Munoz J, Mientjes E, Chen X, Tramp C, Wu J, Yabuuchi A, Chou YF, Buecker C, Krainer A, Willemsen R, Heck AJ, Geijsen N, 2014 DAZL limits pluripotency, differentiation, and apoptosis in developing primordial germ cells. Stem Cell Reports 3, 892–904. [PubMed: 25418731]

Crichton JH, Playfoot CJ, MacLennan M, Read D, Cooke HJ, Adams IR, 2017 Tex19.1 promotes Spo11-dependent meiotic recombination in mouse spermatocytes. PLoS genetics 13, e1006904. [PubMed: 28708824]

Del Moral PM, Warburton D, 2010 Explant culture of mouse embryonic whole lung, isolated epithelium, or mesenchyme under chemically defined conditions as a system to evaluate the molecular mechanism of branching morphogenesis and cellular differentiation. Methods in molecular biology (Clifton, N.J.) 633, 71–79.

Dobin A, Davis CA, Schlesinger F, Drenkow J, Zaleski C, Jha S, Batut P, Chaisson M, Gingeras TR, 2013 STAR: ultrafast universal RNA-seq aligner. Bioinformatics (Oxford, England) 29, 15–21.

Elliott EN, Sheaffer KL, Schug J, Stappenbeck TS, Kaestner KH, 2015 Dnmt1 is essential to maintain progenitors in the perinatal intestinal epithelium. Development 142, 2163–2172. [PubMed: 26023099]

Fan G, Martinowich K, Chin MH, He F, Fouse SD, Hutnick L, Hattori D, Ge W, Shen Y, Wu H, ten Hoeve J, Shuai K, Sun YE, 2005 DNA methylation controls the timing of astrogliogenesis through regulation of JAK-STAT signaling. Development 132, 3345–3356. [PubMed: 16014513]

Hackett JA, Reddington JP, Nestor CE, Dunican DS, Branco MR, Reichmann J, Reik W, Surani MA, Adams IR, Meehan RR, 2012 Promoter DNA methylation couples genome-defence mechanisms to epigenetic reprogramming in the mouse germline. Development 139, 3623–3632. [PubMed: 22949617]

Harfe BD, Scherz PJ, Nissim S, Tian H, McMahon AP, Tabin CJ, 2004 Evidence for an expansion-based temporal Shh gradient in specifying vertebrate digit identities. Cell 118, 517–528. [PubMed: 15315763]

Hargan-Calvopina J, Taylor S, Cook H, Hu Z, Lee SA, Yen MR, Chiang YS, Chen PY, Clark AT, 2016 Stage-Specific Demethylation in Primordial Germ Cells Safeguards against Precocious Differentiation. Dev Cell 39, 75–86. [PubMed: 27618282]

Herriges MJ, Swarr DT, Morley MP, Rathi KS, Peng T, Stewart KM, Morrisey EE, 2014 Long noncoding RNAs are spatially correlated with transcription factors and regulate lung development. Genes Dev 28, 1363–1379. [PubMed: 24939938]

Hines EA, Sun X, 2014 Tissue crosstalk in lung development. J Cell Biochem 115, 1469–1477. [PubMed: 24644090]

Ho UY, Wainwright BJ, 2017 Patched1 patterns Fibroblast growth factor 10 and Forkhead box F1 expression during pulmonary branch formation. Mechanisms of development 147, 37–48. [PubMed: 28939119]

Jackson-Grusby L, Beard C, Possemato R, Tudor M, Fambrough D, Csankovszki G, Dausman J, Lee P, Wilson C, Lander E, Jaenisch R, 2001 Loss of genomic methylation causes p53-dependent apoptosis and epigenetic deregulation. Nat Genet 27, 31–39. [PubMed: 11137995]

Joseph DB, Chandrashekar AS, Abler LL, Chu LF, Thomson JA, Vezina CM, 2019 Epithelial DNA methyltransferase-1 regulates cell survival, growth and maturation in developing prostatic buds. Dev Biol 447, 157–169. [PubMed: 30659795]

Kadzik RS, Cohen ED, Morley MP, Stewart KM, Lu MM, Morrisey EE, 2014 Wnt ligand/Frizzled 2 receptor signaling regulates tube shape and branch-point formation in the lung through control of epithelial cell shape. Proc Natl Acad Sci U S A 111, 12444–12449. [PubMed: 25114215]

Law CW, Chen Y, Shi W, Smyth GK, 2014 voom: Precision weights unlock linear model analysis tools for RNA-seq read counts. Genome biology 15, R29. [PubMed: 24485249]

Lebeche D, Malpel S, Cardoso WV, 1999 Fibroblast growth factor interactions in the developing lung. Mechanisms of development 86, 125–136. [PubMed: 10446271]

Li E, Bestor TH, Jaenisch R, 1992 Targeted mutation of the DNA methyltransferase gene results in embryonic lethality. Cell 69, 915–926. [PubMed: 1606615]

Li SY, Park J, Guan Y, Chung K, Shrestha R, Palmer MB, Susztak K, 2019 DNMT1 in Six2 Progenitor Cells Is Essential for Transposable Element Silencing and Kidney Development. Journal of the American Society of Nephrology : JASN.

Litingtung Y, Lei L, Westphal H, Chiang C, 1998 Sonic hedgehog is essential to foregut development. Nat Genet 20, 58–61. [PubMed: 9731532]

Maatouk DM, Kellam LD, Mann MR, Lei H, Li E, Bartolomei MS, Resnick JL, 2006 DNA methylation is a primary mechanism for silencing postmigratory primordial germ cell genes in both germ cell and somatic cell lineages. Development 133, 3411–3418. [PubMed: 16887828]

Madisen L, Garner AR, Shimaoka D, Chuong AS, Klapoetke NC, Li L, van der Bourg A, Niino Y, Egolf L, Monetti C, Gu H, Mills M, Cheng A, Tasic B, Nguyen TN, Sunkin SM, Benucci A, Nagy A, Miyawaki A, Helmchen F, Empson RM, Knopfel T, Boyden ES, Reid RC, Carandini M, Zeng H, 2015 Transgenic mice for intersectional targeting of neural sensors and effectors with high specificity and performance. Neuron 85, 942–958. [PubMed: 25741722]

Miller LA, Wert SE, Whitsett JA, 2001 Immunolocalization of sonic hedgehog (Shh) in developing mouse lung. The journal of histochemistry and cytochemistry : official journal of the Histochemistry Society 49, 1593–1604.

Pepicelli CV, Lewis PM, McMahon AP, 1998 Sonic hedgehog regulates branching morphogenesis in the mammalian lung. Curr Biol 8, 1083–1086. [PubMed: 9768363]

Rockich BE, Hrycaj SM, Shih HP, Nagy MS, Ferguson MA, Kopp JL, Sander M, Wellik DM, Spence JR, 2013 Sox9 plays multiple roles in the lung epithelium during branching morphogenesis. Proc Natl Acad Sci U S A 110, E4456–4464. [PubMed: 24191021]

Schnatwinkel C, Niswander L, 2013 Multiparametric image analysis of lung-branching morphogenesis. Developmental dynamics : an official publication of the American Association of Anatomists 242, 622–637. [PubMed: 23483685]

Sen GL, Reuter JA, Webster DE, Zhu L, Khavari PA, 2010 DNMT1 maintains progenitor function in self-renewing somatic tissue. Nature 463, 563–567. [PubMed: 20081831]

Sheaffer KL, Kim R, Aoki R, Elliott EN, Schug J, Burger L, Schubeler D, Kaestner KH, 2014 DNA methylation is required for the control of stem cell differentiation in the small intestine. Genes & development 28, 652–664. [PubMed: 24637118]

Shin YH, Ren Y, Suzuki H, Golnoski KJ, Ahn HW, Mico V, Rajkovic A, 2017 Transcription factors SOHLH1 and SOHLH2 coordinate oocyte differentiation without affecting meiosis I. J Clin Invest 127, 2106–2117. [PubMed: 28504655]

Shu W, Yang H, Zhang L, Lu MM, Morrisey EE, 2001 Characterization of a new subfamily of winged-helix/forkhead (Fox) genes that are expressed in the lung and act as transcriptional repressors. J Biol Chem 276, 27488–27497. [PubMed: 11358962]

Snitow M, Lu M, Cheng L, Zhou S, Morrisey EE, 2016 Ezh2 restricts the smooth muscle lineage during mouse lung mesothelial development. Development 143, 3733–3741. [PubMed: 27578795]

Snitow ME, Li S, Morley MP, Rathi K, Lu MM, Kadzik RS, Stewart KM, Morrisey EE, 2015 Ezh2 represses the basal cell lineage during lung endoderm development. Development 142, 108–117. [PubMed: 25516972]

Swarr DT, Morrisey EE, 2015 Lung endoderm morphogenesis: gasping for form and function. Annu Rev Cell Dev Biol 31, 553–573. [PubMed: 26359777]

Takizawa T, Nakashima K, Namihira M, Ochiai W, Uemura A, Yanagisawa M, Fujita N, Nakao M, Taga T, 2001 DNA methylation is a critical cell-intrinsic determinant of astrocyte differentiation in the fetal brain. Dev Cell 1, 749–758. [PubMed: 11740937]

Tsui S, Dai T, Roettger S, Schempp W, Salido EC, Yen PH, 2000 Identification of two novel proteins that interact with germ-cell-specific RNA-binding proteins DAZ and DAZL1. Genomics 65, 266–273. [PubMed: 10857750]

Wan H, Liu C, Wert SE, Xu W, Liao Y, Zheng Y, Whitsett JA, 2013 CDC42 is required for structural patterning of the lung during development. Dev Biol 374, 46–57. [PubMed: 23219958]

Wang X, Wang Y, Snitow ME, Stewart KM, Li S, Lu M, Morrisey EE, 2016a Expression of histone deacetylase 3 instructs alveolar type I cell differentiation by regulating a Wnt signaling niche in the lung. Developmental biology 414, 161–169. [PubMed: 27141870]

Wang Y, Frank DB, Morley MP, Zhou S, Wang X, Lu MM, Lazar MA, Morrisey EE, 2016b HDAC3-Dependent Epigenetic Pathway Controls Lung Alveolar Epithelial Cell Remodeling and Spreading via miR-17–92 and TGF-beta Signaling Regulation. Dev Cell 36, 303–315. [PubMed: 26832331]

Wang Y, Tian Y, Morley MP, Lu MM, Demayo FJ, Olson EN, Morrisey EE, 2013 Development and regeneration of Sox2+ endoderm progenitors are regulated by a Hdac1/2-Bmp4/Rb1 regulatory pathway. Dev Cell 24, 345–358. [PubMed: 23449471]

Weaver M, Dunn NR, Hogan BL, 2000 Bmp4 and Fgf10 play opposing roles during lung bud morphogenesis. Development 127, 2695–2704. [PubMed: 10821767]

Whitsett JA, Kalin TV, Xu Y, Kalinichenko VV, 2019 Building and Regenerating the Lung Cell by Cell. Physiol Rev 99, 513–554. [PubMed: 30427276]

Yao C, Carraro G, Konda B, Guan X, Mizuno T, Chiba N, Kostelny M, Kurkciyan A, David G, McQualter JL, Stripp BR, 2017 Sin3a regulates epithelial progenitor cell fate during lung development. Development (Cambridge, England) 144, 2618–2628.

- Loss of *Dnmt1* leads to precocious distalization and loss of proximal endoderm
- Dnmt1 is required for branching morphogenesis and epithelial-mesenchymal crosstalk
- Epithelial shape and polarity are disrupted in Dnmt1 deficient lungs
- Dnmt1 mutants exhibit premature activation of the AT2 cell transcriptional program

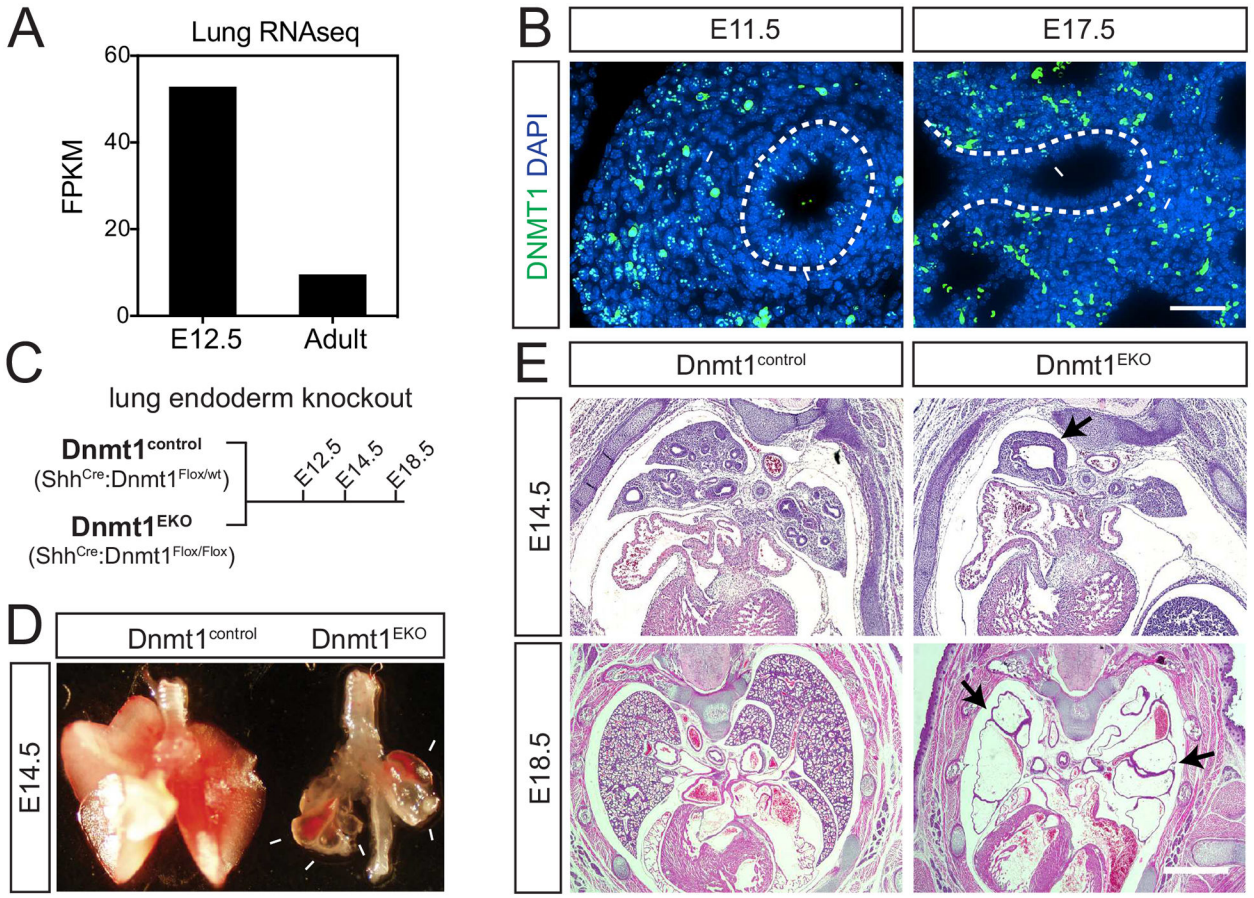

Figure 1: Endodermal Dnmt1 is required for lung development.

(A) RNA-seq analysis reveals that *Dnmt1* expression is enriched in E12.5 compared to adult lungs (units reflected in fragments per kilobase of transcript per million mapped reads) (B) Immunohistochemical staining for Dnmt1 at E11.5 and E17.5 demonstrates its presence in both the endodermal and mesenchymal compartments prenatally (dashed lines demarcate endoderm)(scale bar: 50μm). (C) Experimental schematic of developmental time points assessed in endodermal *Dnmt1* knockout model. (D) Comparison of $Dnmt1^{EKO}$ and $Dnmt1^{control}$ lungs at E14.5 (white arrows indicate cystic buds). (E) Hematoxylin and eosin (H&E) staining of histological sections of $Dnmt1^{EKO}$ lungs demonstrate defective developmental progression by E14.5 and failure by E18.5 (black arrows point to cystic buds) (scale bar: 500μm).

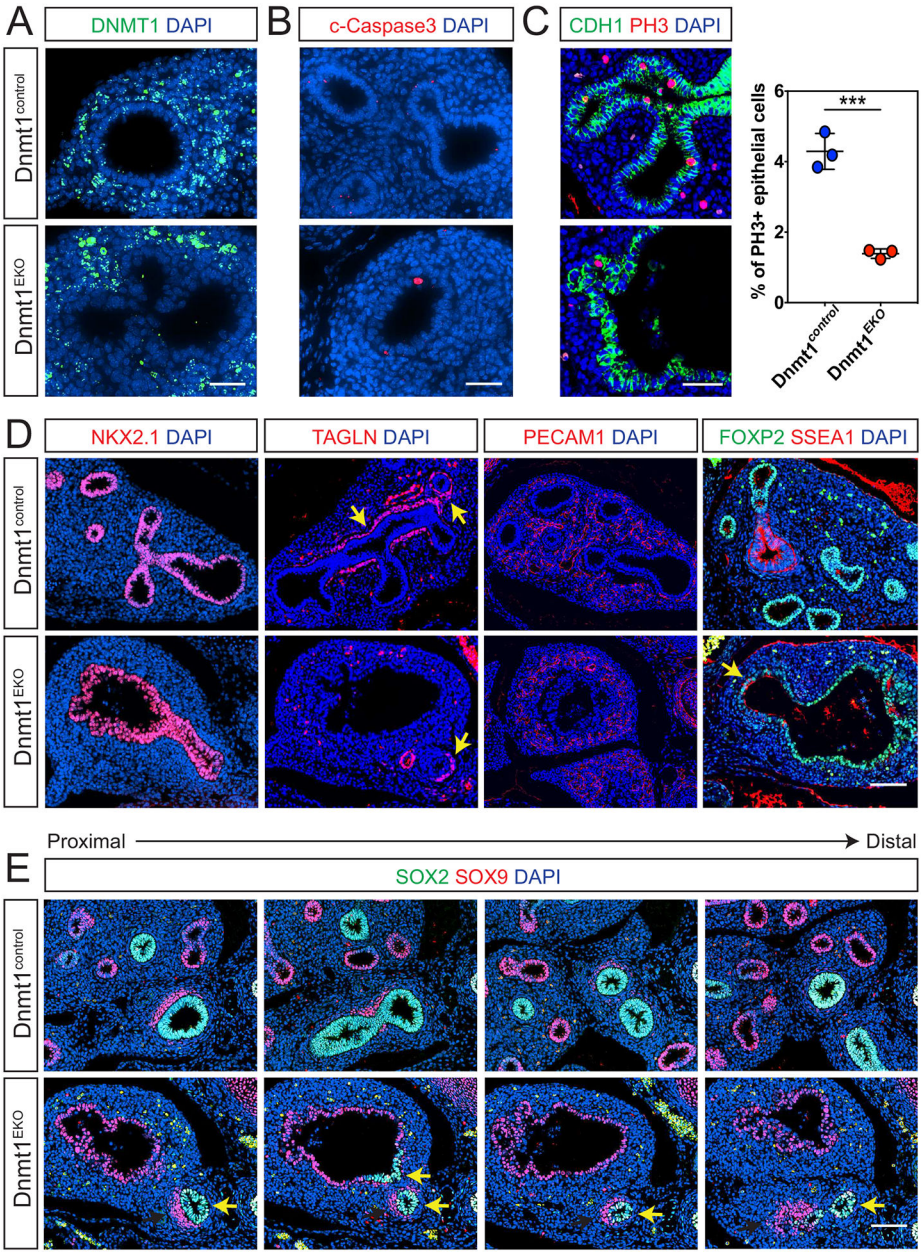

Figure 2: Endodermal loss of *Dnmt1* disrupts proximal-distal patterning.

(A) Immunohistochemical staining for Dnmt1 indicates it is lost in the lung endoderm at E14.5 in Dnmt1^{EKO} lungs (dashed lines demarcate endoderm)(scale bar: 50μm). (B) Immunohistochemical staining for cleaved caspase-3 indicates that cell death is increased in Dnmt1^{EKO} lungs at E14.5 (dashed lines demarcate endoderm)(scale bar: 50μm). (C) Quantification of epithelial proliferation by assessment of Cdh1 and Phosphohistone H3 double positive cells shows a significant decrease in endodermal proliferation in Dnmt1^{EKO} lungs. Cdh1 stain reveals perturbed epithelial cell shape and aberrant twisting of epithelial buds in Dnmt1^{EKO} lungs (scale bar: 50μm, student's twotailed t-test, P<0.001). (D) Immunohistochemical staining for Nkx2.1 shows lung epithelial cell specification in both Dnmt1^{EKO} and Dnmt1^{control} lungs. Staining for smooth muscle marker Tagln (smooth

muscle surrounding vessels is marked by white arrows, smooth muscle surrounding airways is marked by yellow arrows) and endothelial cell marker Pecam1 demonstrates proper differentiation and localization of mesoderm-derived structures in Dnmt1^{EKO} lungs. Staining for proximal endoderm marker SSEA1 as well as distal endoderm marker Foxp2 reveals perturbed proximal/distal patterning in Dnmt1^{EKO} lungs (proximal endoderm is marked by a yellow arrow, distal endoderm is marked by a white arrow) (scale bar: 100μm). (E) Immunohistochemical staining for Sox2 and Sox9 in a series of sections from proximal to distal shows expansion of the distal endoderm compartment (proximal endoderm is marked by yellow arrows, distal endoderm is marked by white arrows, cartilage progenitors are marked by black arrows)(scale bar: 100μm).

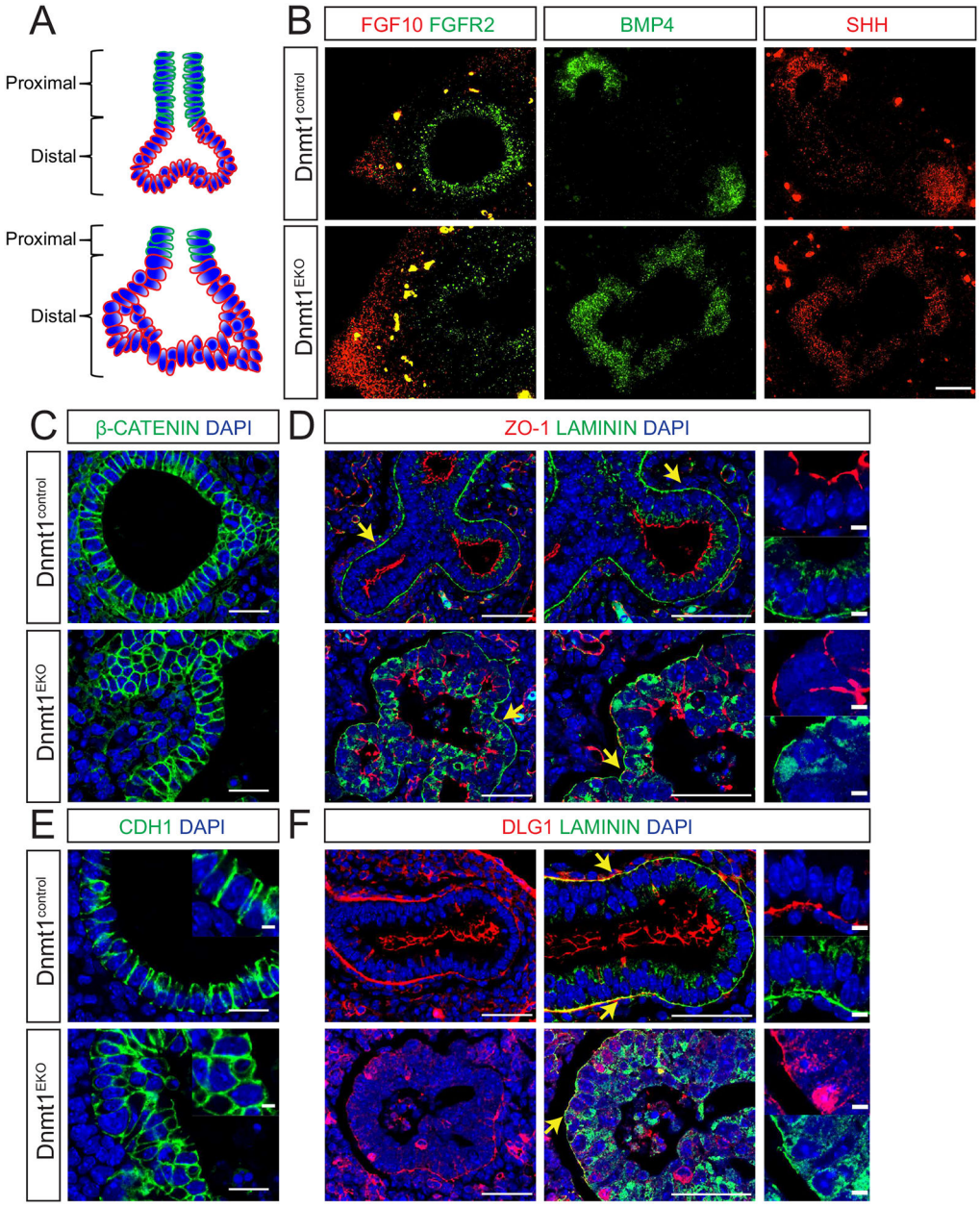

Figure 3: Dnmt1 is essential to maintain epithelial-mesenchymal crosstalk and epithelial polarity.

(A) A model of Dnmt1^{control} (top) vs. Dnmt1^{EKO} (bottom) lungs demonstrates the expansion of the distal compartment, perturbed epithelial cell shape, and abnormal twisting of epithelial buds in Dnmt1^{EKO} lungs. (B) RNA fluorescence *in situ* hybridization reveals a decrease in *Fgfr2* expression in Dnmt1 mutant endoderm and an expansion of *Fgf10* expression in the mesoderm. *Bmp4* and *Shh* expression are expanded in Dnmt1^{EKO} lungs consistent with expansion of the distal endodermal compartment (white dashed line demarcates endoderm, white arrows indicate distal buds of the endoderm) (scale bar: 50μm). (C) Immunohistochemistry for β-catenin reveals loss of characteristic columnar shape of Dnmt1 mutant epithelial cells (scale bars: 25μm). (D) Immunohistochemistry for ZO-1 (white arrows) and laminin (yellow arrows) shows the proper localization of ZO-1 to the

apical membrane of Dnmt1^{control} endodermal cells and deposition of laminin in the basement membrane compared to ectopic localization of ZO-1 to the lateral and basal membranes of Dnmt1^{EKO} endodermal cells and abnormal localization of laminin despite also being present in the basement membrane (scale bars from left to right: 50μm, 50 μm, 5 μm). (E) Immunohistochemical staining for Cdh1 demonstrates perturbed epithelial cell shape and aberrant localization of Cdh1 protein to the apical membrane of Dnmt1^{EKO} endodermal cells (scale bars: 25μm). (F) Immunohistochemistry for Dlg1 (white arrows) and laminin (yellow arrows) shows the proper localization of Dlg1 to the basal membrane of Dnmt1^{control} endodermal cells and deposition of laminin in the basement membrane compared to strong cytosolic and abnormal lateral membrane staining of Dlg1 in Dnmt1^{EKO} endodermal cells. Laminin is again present in the basement membrane and is abnormally localized in Dnmt1^{EKO} endodermal cells (scale bars from left to right: 50μm, 50 μm, 5 μm).

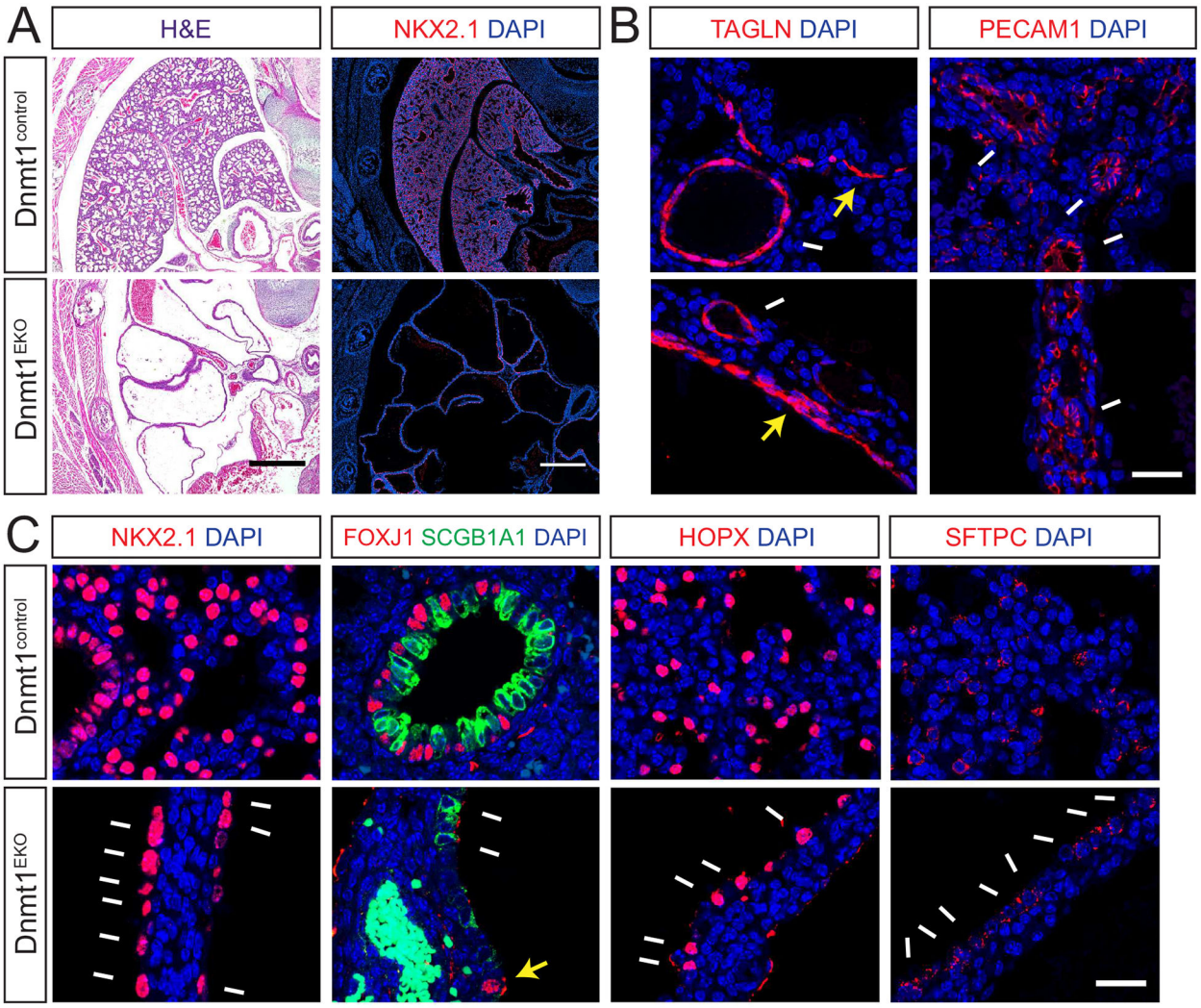

Figure 4: Loss of *Dnmt1* impacts endodermal differentiation.

(A) H&E and immunohistochemical staining for Nkx2.1 and DAPI reveal cystic sacs in place of a normal branched network with a paucity of Nkx2.1 cells in Dnmt1^{EKO} lungs (scale bars: 500μm). (B) Immunohistochemical staining for Tagln and Pecam1 demonstrate E18.5 lungs are vascularized and that large vessels are surrounded with smooth muscle (vessels are marked by white arrows). Smooth muscle also lines the large cysts in Dnmt1^{EKO} lungs (yellow arrow (top image) marks smooth muscle surrounding an airway yellow arrow (bottom image) marks smooth muscle lining cystic lung buds)(scale bars: 25μm). (C) A magnified image of immunohistochemistry for Nkx2.1 shows epithelial cells are present at E18.5 (first image marked by white arrows). Airway epithelial cell types marked by Scgb1a1 and Foxj1 (second image, white and yellow arrows respectively) are rare in Dnmt1^{EKO} lungs, while alveolar type 1 cells marked by Hopx (third image, white arrows) and alveolar type 2 cells marked by Sftpc (fourth image, white arrows) are more common (scale bar: 25μm).

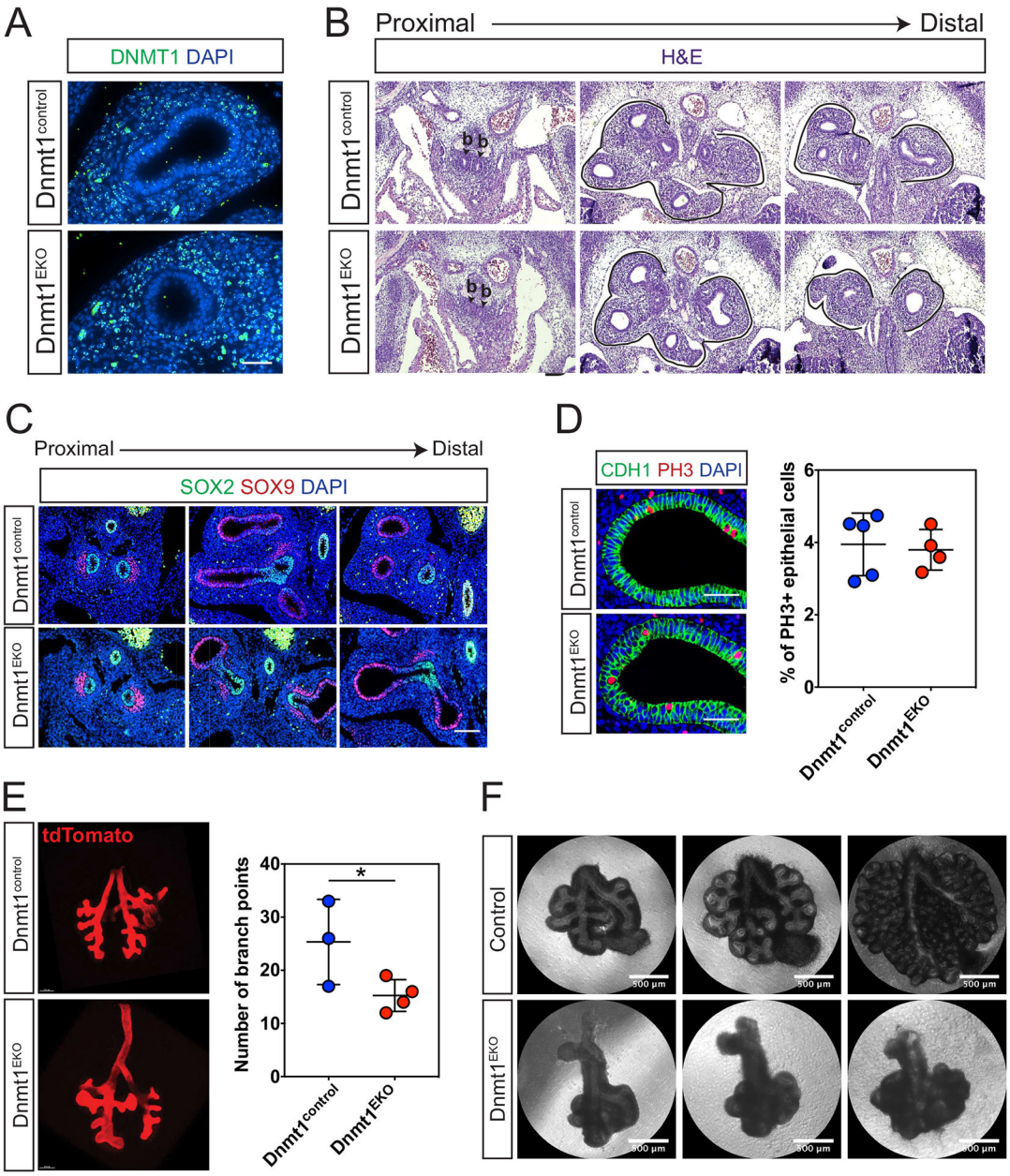

Figure 5: Dnmt1 is required for proper branching morphogenesis.

(A) Dnmt1 protein is lost in the lung endoderm in Dnmt1^{EKO} lungs at E12.5 (dashed lines demarcate endoderm)(scale bar: 50μm). (B) *Dnmt1^{EKO}* lungs display a subtle branching defect by H&E staining (black lines demarcate endoderm) (scale bar: 100μm). (C) Immunohistochemistry for Sox2 and Sox9 reveal no major disturbance of the proximal-distal axis at E12.5 (scale bar: 100μm). (D) Quantification of epithelial proliferation by assessment of Cdh1 and Phosphohistone H3 double positive cells shows no significant difference between Dnmt1^{EKO} and Dnmt1^{control} lungs (scale bar: 50μm, student's two-tailed t-test, P>0.05). (E) Branch point analysis of E12.5 lungs demonstrates a statistically significant decrease in branching in Dnmt1^{EKO} lungs (scale bars: 150μm, student's one-tailed t-test, P<0.05). (F) Still images from *ex vivo* live imaging of E11.5 lungs at 0, 24, and

72 hours of culture reveal that the disturbed branching patterns and formation of cystic sacs in Dnmt1^{EKO} lungs are lung intrinsic defects. White arrow indicates loss of a domain branch in Dnmt1^{EKO} lungs (scale bar: 500μm).

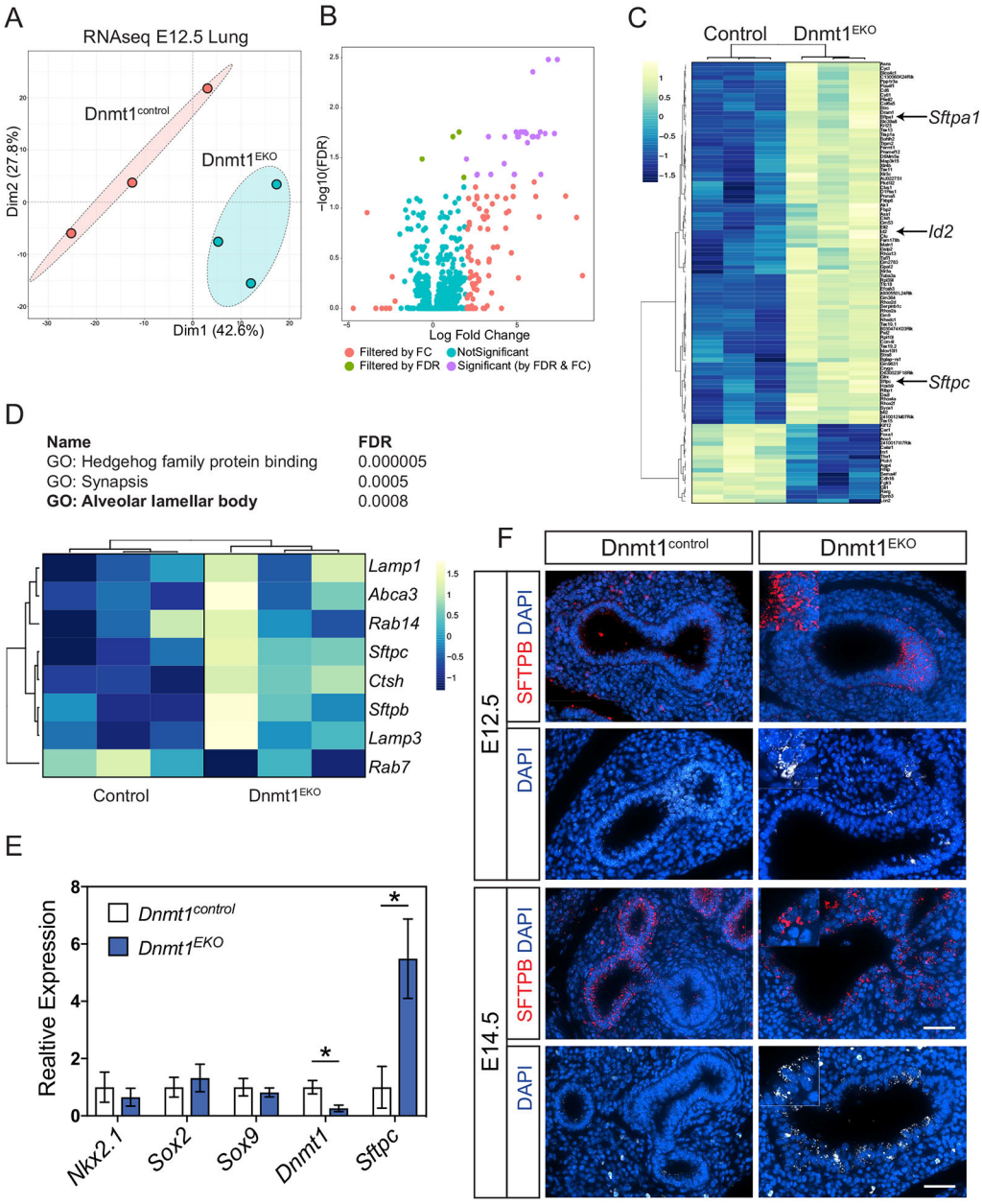

Figure 6: *Dnmt1* knockout lungs exhibit precocious AT2 differentiation signature.

(A) PCA demonstrates E12.5 Dnmt1^{EKO} and control lungs cluster separately. (B/C) Visualization of differentially expressed transcripts in Dnmt1^{EKO} versus control lungs by volcano plot and heat map show distal endoderm markers and surfactant genes enriched in Dnmt1^{EKO} lungs. (D/E) GO category analysis reveals alveolar lamellar body related genes to be among the most up-regulated in Dnmt1^{EKO} lungs. (F) qPCR verification of Nkx2.1, Sox2, and Sox9 expression confirms no significant difference in expression between Dnmt1^{EKO} and control lungs, while expression of *Dnmt1* is significantly decreased and Sftpc is significantly enriched in Dnmt1^{EKO} lungs. (G) Endodermal cells stain positive for Sftpb and Sftpc protein in Dnmt1^{EKO} lungs at E12.5. At E14.5 Sftpb staining is expanded

throughout the endoderm of Dnmt1^{EKO} lungs and Sftpc staining is more abundant in Dnmt1^{EKO} compared to Dnmt1^{control} lungs (scale bar: 50μm).